BMES
BIOMEDICAL ENGINEERING SOCIETY™
www.bmes.org

CrossMark

In Vivo Contrast-Enhanced Cone Beam CT Provides Quantitative Information on Articular Cartilage and Subchondral Bone

Katariina A. H. Myller [1,2] Mikael J. Turunen,[1] Juuso T. J. Honkanen,[1,2] Sami P. Väänänen [1,2] Jarkko T. Iivarinen,[1] Jari Salo,[3,4] Jukka S. Jurvelin,[1,2] and Juha Töyräs[1,2]

[1]Department of Applied Physics, University of Eastern Finland, P.O. Box 1627, 70211 Kuopio, Finland; [2]Diagnostic Imaging Center, Kuopio University Hospital, P.O. Box 100, 70029 Kuopio, Finland; [3]Orthopaedics and Traumatology Clinic, Mehiläinen, Pohjoinen Hesperiankatu 17 C, 00260 Helsinki, Finland; and [4]Kuopio Musculoskeletal Research Unit (KMRU), Surgery, Institute of Clinical Medicine, University of Eastern Finland, 70211 Kuopio, Finland

Associate Editor Michael R. Torry oversaw the review of this article.

Abstract—In post-traumatic osteoarthritis, both articular cartilage and subchondral bone undergo characteristic pathological changes. This study investigates potential of delayed cone beam computed tomography arthrography (dCBCTa) to simultaneously detect variations in cartilage and subchondral bone. The knees of patients ($n = 17$) with suspected joint injuries were imaged using a clinical CBCT scanner at 5 and 45 min after the intra-articular injection of anionic contrast agent (Hexabrix™) with hydroxyapatite phantoms around the knee. Normalized attenuation (i.e., contrast agent partition, an indicator of tissue composition) in cartilage, bone mineral density (BMD) in subchondral bone plate (SBP), subchondral bone and trabecular bone, and thicknesses of SBP and cartilage were determined. Lesions of cartilage were scored using International Cartilage Repair Society (ICRS) grading. Normalized attenuation in the delayed image ($t = 45$ min) increased along the increase of ICRS grade ($p = 0.046$). Moreover, BMD was significantly higher in SBPs under damaged cartilage (ICRS = 1–2 or ICRS $\geq$ 3; $p = 0.047$ and $p = 0.038$, respectively) than in SBP under non-injured tissue (ICRS = 0). For the first time, dCBCTa enabled the detection of articular cartilage injuries and subchondral bone alterations simultaneously *in vivo*. Significant relations between ICRS grading and both cartilage and bone parameters suggest that dCBCTa has potential for quantitative imaging of the knee joint.

Keywords—Computed tomography, Knee joint, Osteoarthritis, Quantitative imaging, Contrast agent.

INTRODUCTION

Osteoarthritis (OA) is a common joint disease that causes degeneration of articular cartilage but also affects subchondral bone.[5,24] Lesions in the cartilage collagen network, typically found after mechanical traumas, may trigger the progression of osteoarthritis (OA).[5,7] In order to prevent further progression of initial tissue changes, as well as to enable remedial (e.g. surgical repair) treatments,[7] early detection of tissue alterations in joint structures is essential. As it is still uncertain whether the OA is initiated by changes in cartilage or subchondral bone,[24,26] significant interest in alterations of subchondral bone has been transpired.[2,3,10,19,22,24,35] In OA, stress-induced remodeling may stiffen the subchondral bone,[10,24] leading to cartilage overloading and, subsequently, to tissue degeneration. Further, bone related changes also include sclerosis, osteophytes and osteochondral cysts.[6,19] The coupling between the changes in cartilage and subchondral bone during OA progression is, nevertheless, still under debate.

Traditional methods used for the detection of OA related alterations and injuries include magnetic resonance imaging (MRI), radiography [e.g. X-ray and computed tomography (CT)], clinical examination and arthroscopy. Clinical MRI serves as a common approach for soft tissue imaging, however, the resolution disables detection of small tissue alterations. Its capability to visualize bone is also limited. Furthermore, MRI suffers from relatively high imaging costs and limited accessibility in acute traumatic incidents. Radiography has an advantage to image bony structures with high resolution, and CT has significantly

Address correspondence to Katariina A. H. Myller, Department of Applied Physics, University of Eastern Finland, P.O. Box 1627, 70211 Kuopio, Finland. Electronic mail: katariina.myller@uef.fi, mikael.turunen@uef.fi, juuso.honkanen@uef.fi, sami.vaananen@uef.fi, jarkko.iivarinen@iki.fi, jari.salo@mehilainen.fi, jukka.jurvelin@uef.fi, juha.toyras@uef.fi

shorter acquisition time than clinical MRI. However, detection of subtle cartilage defects is implausible due to poor soft tissue contrast in X-ray imaging. Arthroscopic imaging is the gold standard method for evaluation of cartilage injuries. However, the method is invasive and the diagnosis subjective with large inter- and intra-observer variabilities.[30]

Delayed CT arthrography (dCTa), an analogous method to delayed gadolinium enhanced MRI of cartilage (dGEMRIC),[11] may overcome some of the limitations and enable simultaneous detection of tissue alterations of bone and cartilage. The method utilizes anionic contrast agents that diffuse into cartilage in an inverse proportion to the spatial proteoglycan (PG) content of the cartilage.[27] As the loss of negatively charged PGs is one of the first signs of cartilage degeneration,[21] dCTa may detect this change. Moreover, the diffusion of the contrast agents depends on the integrity and crosslinking of collagen network in cartilage.[15,17] Hence, dCTa can also detect fresh cartilage lesions already before depletion of PGs.[14]

Modern extremity cone beam computed tomography (CBCT) scanners provide lower radiation doses and potentially higher resolution than clinical CT scanners.[25] CBCT has been shown to be an advantageous and feasible method to observe cartilage alterations *in vivo*.[16] Moreover, our recent study showed that CBCT is suited for analysis of local bone mineral density (BMD) and its volumetric distribution.[32] This may provide an advantage as subchondral bone typically experiences changes in OA.[19] Additionally, CBCT enables the determination of the volumes and thicknesses of cartilage and subchondral bone plate. Results of the previous *in vitro* and *in vivo* studies on contrast-enhanced CT imaging of cartilage[13–17,27,29] are encouraging, however, the applicability of the technique to simultaneously analyze both tissues has not been confirmed. Indeed, simultaneous CBCT analysis of contrast agent partition in cartilage and BMD of underlying bone would enable more comprehensive evaluation of the knee joint.

The present study evaluates the *in vivo* potential of delayed CBCT arthrography (dCBCTa) by assessing if OA related cartilage and bone alterations could be detected quantitatively and simultaneously from the dCBCTa images. Local variations in volumetric bone mineral density (vBMD) and normalized attenuations (i.e., contrast agent partitions), as well as the thicknesses of cartilage and subchondral bone plate (SBP) are determined. As a study hypothesis, the variations and changes in the properties of subchondral bone and cartilage are inter-related and can be quantitatively detected *in vivo* using a clinical CBCT scanner.

MATERIALS AND METHODS

Patients

The study protocol was reviewed by the Ethical Committee of Kuopio University Hospital, Kuopio, Finland (Favourable Opinion No: 54/2011) and the study adhered the Declaration of Helsinki. Patients with suspected knee joint injuries ($n = 17$, age 32–65, 9 women and 8 men) were voluntarily enrolled in delayed CBCT arthrography study by a clinician's referral. Only patients, whose knees showed no signs of inflammation or infection, were selected to this study.

CBCT Imaging

One knee of each patient ($n = 17$) was imaged using a peripheral CBCT scanner (Verity, Planmed Oy, Finland) in a private clinic (Mehiläinen, Helsinki). Patients were imaged at 5 min and 45 min after the intra-articular injection of the anionic contrast agent ($V = 20$ mL, $q = -1$, $M = 1269$ g/mol, 320 mg iodine/mL, Hexabrix^{TM}, Mallinckrodt Inc., St. Louis, MO, USA) diluted to half of its concentration using saline. Based on our previous study,[32] four custom made hydroxyapatite phantoms (184.2; 315.1; 593.7; 820.1 mg/cm^3) were placed around the leg, at the height of the proximal tibia. CBCT imaging was carried out using the tube voltage of 96 kV, 54 mAs, and voxel size of $200 \times 200 \times 200$ μm^3. Flexion and extension of the leg was gently repeated for a few minutes prior to the imaging sessions to ensure an even distribution of the contrast agent within the joint capsule.

Image Analysis

The delayed ($t = 45$ min) three-dimensional (3D) image stack was co-registered with the arthrographic ($t = 5$ min) stack separately according to patella, femur and tibia using Analyze software (Analyze 10.0, Analyze direct, Inc., KS, USA). Cylindrical volumes-of-interest (VOIs) ($d = 20$ mm) were selected from six different anatomical sites (femoral lateral condyle (FLC), femoral medial condyle (FMC), femoral groove (FG), patella (PAT), tibial lateral condyle (TLC), and tibial medial condyle (TMC)) (Fig. 1b). In each VOI ($n = 102$), cartilage, subchondral bone plate (SBP), subchondral bone (SB) and trabecular bone (TB) were segmented manually (Seg3D 2.2.1, Scientific Computing and Imaging Institute, University of Utah, UT, USA) (Fig. 1c). In addition, synovial fluid (SF) VOIs were segmented in lateral and medial tibiofemoral condyles and patellofemoral groove from both image stacks. As the cartilage surface could be accu-
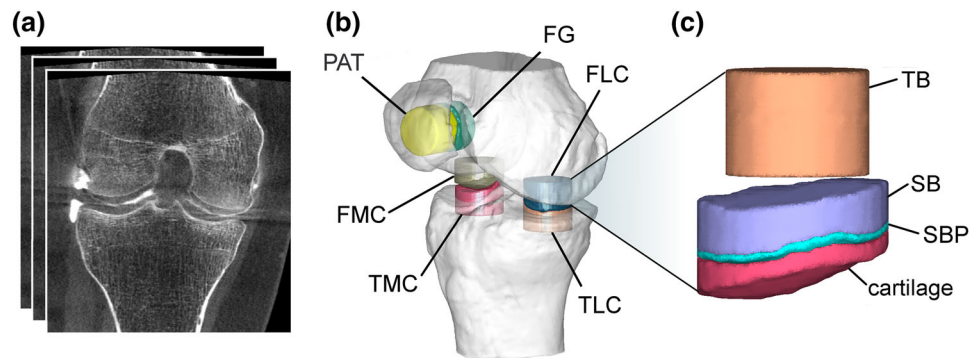
FIGURE 1. (a) Contrast-enhanced CBCT images of human knee joint (coronal slices). (b) 3D-render of the bones of the knee illustrating the anatomical sites examined in this study: FLC, femoral lateral condyle; FMC, femoral medial condyle; FG, femoral groove; PAT, patella; TLC, tibial lateral condyle; TMC, tibial medial condyle. (c) Segmented VOIs of FLC, similar to the other anatomical sites. TB, trabecular bone; SB, subchondral bone; SBP, subchondral bone plate.

rately visualized in arthrographic images, they were used for the segmentation of cartilage VOIs. Cartilage lesions in the images, containing only the contrast agent, were excluded from quantitative analysis. Furthermore, cysts and hollow parts were excluded from bone VOIs to include only bone tissue for analysis. Very thin SBPs (≤1 pixels) were excluded from the analysis,[23] thus decreasing the SBP sample size to 74. Voxels at the cartilage surfaces or at the interfaces of multiple tissues were also excluded in order to minimize the partial volume effect. The co-registering of the arthrographic and delayed image stacks enabled the use of same segmented masks for analysis of both 5 and 45 min image stacks. MATLAB (Matlab, R2014a, MathWorks Inc., Natick, MA, USA) was used for data analysis.

Quantitative Analyses

Hydroxyapatite phantoms were used as calibrators to quantify vBMDs at bone VOIs. Therefore, the vBMDs of phantoms were determined using dual-energy X-ray absorptiometry (GE Healthcare Lunar iDXA, Madison, WI, USA). In CBCT images, the full phantom volume, except the most exterior parts of the phantom, was used to determine the mean X-ray attenuation in the phantom material. In each image, vBMD was calibrated using linear fitting between mean X-ray attenuation and vBMD values of the phantoms. Then, the vBMDs at VOIs (SBP, SB, and TB) were determined using the mean X-ray attenuation within each VOI.

To obtain the normalized attenuation in cartilage, the mean values of X-ray attenuation in each cartilage VOI were calculated and normalized with that of adjacent SF VOIs in the same image by dividing the cartilage X-ray attenuation with the SF X-ray attenuation. The normalized attenuations of arthrographic ($t = 5$ min) and delayed ($t = 45$ min) images were

used in further analyses. In addition, the thicknesses of SBP and cartilage were calculated by dividing the VOI volume with the cross-sectional area of the VOI.

ICRS Scoring

Arthrographic CBCT images were scored using the modified ICRS (International Cartilage Research Society) grading system.[16] Scoring was performed by two individuals who scored lesions in blind-coded images of cartilage VOIs three times in random order with a minimum of four hours between the scorings. Mean values, rounded to the closest integer, of the scorings of each cartilage VOI were used in further analyses. Inter-observer standard deviation was 0.24.

Statistical Analysis

SPSS (SPSS, v. 21.0.0.0., Chicago, IL, USA) was used for statistical analyses. The limit for statistical significance was set to $p < 0.05$ and confidence interval to 95%. Wilcoxon signed rank test was used to test differences in normalized attenuation and vBMDs between the anatomical sites. Mann–Whitney U-test was used to examine differences in normalized attenuations of intact to lightly damaged (ICRS ≤ 1) and injured (ICRS ≥ 2) cartilages at different anatomical sites. Generalized linear Mixed Model analysis was used to compare the mean values of normalized attenuations of the same categories (ICRS ≤ 1 and ICRS ≥ 2). The same analysis was used to study differences in vBMDs of SBP, SB and TB at intact (ICRS = 0), damaged (ICRS = 1–2) and severely damaged (ICRS ≥ 3) sites. The significance of difference between the normalized attenuations in cartilages with different ICRS grading were evaluated using the linear Mixed Model analysis. The linear Mixed Model was constructed using the normalized attenuation in dCBCTa images as a static effect and patient as a

random effect. Correlations were determined using Spearman's rho (ρ) correlation coefficient.

RESULTS

The normalized attenuation ($t = 45$ min) of intact to lightly damaged (ICRS ≤ 1) cartilage varied between anatomical sites (Fig. 2). The normalized attenuation ($t = 45$ min) was significantly higher ($p = 0.003$, all anatomical sites, $n = 102$) in injured cartilage (ICRS ≥ 2) than in intact or lightly damaged cartilage (ICRS ≤ 1) (Fig. 2). Furthermore, when analyzing the arthrographic images ($t = 5$ min) similarly as delayed ($t = 45$ min) images (Fig. 2), the normalized attenuation at 5 min was significantly greater ($p = 0.021$, all anatomical sites, $n = 102$) in cartilage VOIs including lesions (ICRS ≥ 2) than in intact or lightly damaged (ICRS ≤ 1) VOIs.

Significant differences in vBMD of intact SBP, SB and TB between the anatomical sites were found (Table 1). Further, vBMD of SBP was significantly greater in damaged (ICRS = 1–2) and severely damaged (ICRS ≥ 3) sites compared with that at intact (ICRS = 0) sites ($p = 0.047$ and $p = 0.038$, respectively) (Fig. 3). No significant differences in vBMD between the intact and damaged or severely damaged sites were found in SB ($p = 0.217$ and $p = 0.104$, respectively) or TB ($p = 0.306$ and $p = 0.097$, respectively).

The ICRS grade of a lesion was a significant predictor ($p = 0.046$, $n = 102$) of the normalized attenuation in cartilage ($t = 45$ min) (Fig. 4). SBP mineral density and normalized attenuation in cartilage ($t = 5$ min and $t = 45$ min) correlated positively with ICRS grades (Table 2). When considering only the
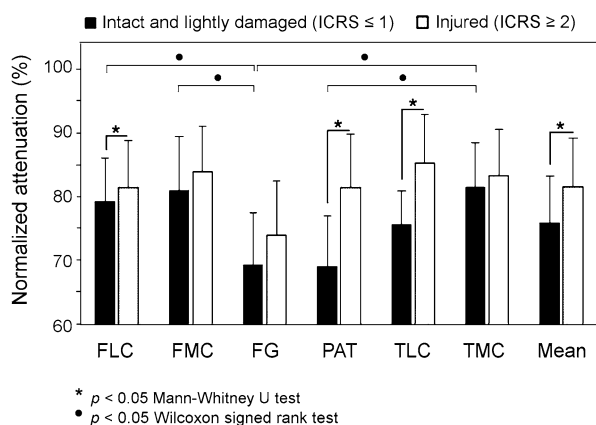
TABLE 1. vBMDs (mg/cm^3, mean ± SD) of subchondral bone plate, subchondral bone, and trabecular bone at intact sites (ICRS ≤ 1). Only values at intact sites were compared to investigate anatomical variation of vBMD.

	Subchondral bone plate ($n = 27$)	Subchondral bone ($n = 36$)	Trabecular bone ($n = 36$)
FLC	532 ± 79	373 ± 77	298 ± 79
FMC	571 ± 76	425 ± 76	308 ± 65
FG	673 ± 91	515 ± 106	321 ± 88
PAT	-	626 ± 221	330 ± 83
TLC	561 ± 93	355 ± 110	197 ± 83
TMC	637 ± 82	519 ± 128	297 ± 102

$p < 0.5$ with values connected with the bracket (Wilcoxon signed rank test); FLC, femoral lateral condyle; FMC, medial condyle of femur; FG, femoral groove; PAT, patella; TLC, lateral condyle of tibia; TMC, medial condyle of tibia. Very thin SBPs were excluded from the set decreasing the number of samples to 27.
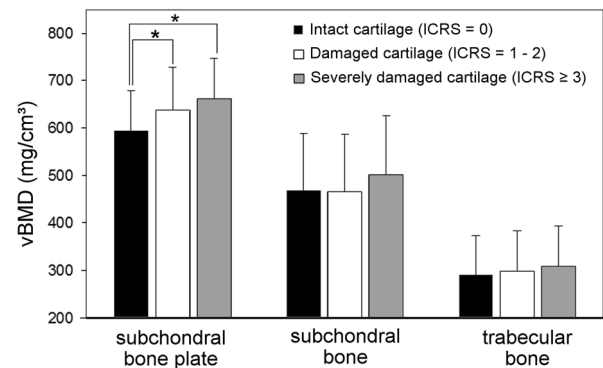

FIGURE 3. Volumetric bone mineral densities (vBMD, mg/cm^3, mean ± SD) of subchondral bone plate, subchondral bone, and trabecular bone ($n = 74$, $n = 102$, $n = 102$, respectively) under severely damaged (ICRS ≥ 3), damaged (ICRS = 1–2) and intact (ICRS = 0) cartilage. Statistically significant ($p < 0.05$) differences are indicated with * (generalized linear Mixed Model analysis).

FIGURE 2. Normalized attenuation (i.e., contrast agent partition) at 45 min after ioxaglate injection in intact and lightly damaged (ICRS ≤ 1) and injured (ICRS ≥ 2) cartilage VOIs of different anatomical sites. FLC, femoral lateral condyle; FMC, femoral medial condyle; FG, femoral groove; PAT, patella; TLC, tibial lateral condyle; TMC, tibial medial condyle.
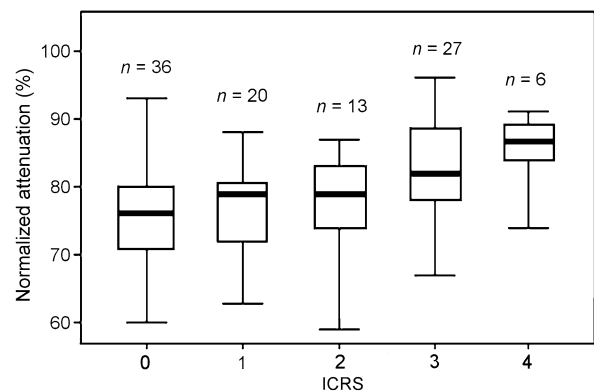

FIGURE 4. Normalized attenuation ($t = 45$ min) in articular cartilage ($n = 102$) as a function of ICRS grading. The increasing trend is statistically significant ($p = 0.046$, linear Mixed Model).

TABLE 2. Spearman rank correlation coefficients (ρ) of bone and cartilage parameters.

	SB mineral density	TB mineral density	SBP thickness	CA_5	CA_{45}	$CA_{45} - CA_5$	Cartilage thickness	ICRS
SBP mineral density	**0.796****	**0.402****	**0.366****	−0.031	−0.007	0.045	−0.093	**0.283***
SB mineral density	–	**0.681****	**0.228***	−0.049	−0.063	−0.071	−0.161	0.133
TB mineral density		–	−0.114	−0.047	0.095	0.111	−0.153	0.112
SBP thickness			–	**0.253***	0.070	−0.185	−0.057	0.103
CA_5				–	**0.533****	**−0.268****	**−0.304****	**0.305****
CA_{45}					–	**0.619****	**−0.374****	**0.363****
$CA_{45} - CA_5$						–	−0.115	0.120
Cartilage thickness							–	**−0.319***

Statistically significant values are given in bold.
* $p < 0.05$, ** $p < 0.01$.
SBP, subchondral bone plate; SB, subchondral bone; TB, trabecular bone; CA_5, normalized attenuation ($t = 5$ min) in cartilage; CA_{45}, normalized attenuation ($t = 45$ min) in cartilage.
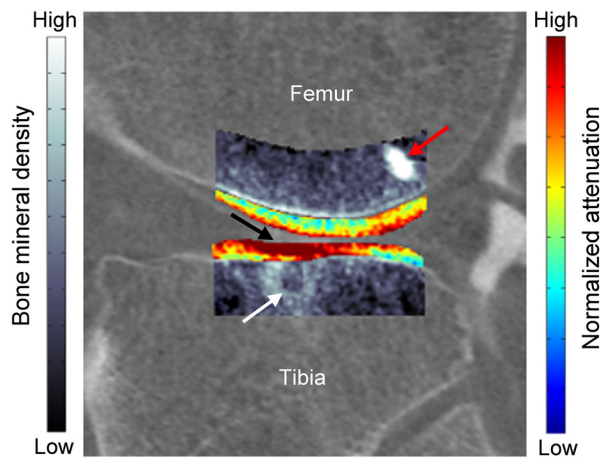

FIGURE 5. **Quantitative distribution of volumetric bone mineral density and normalized attenuation ($t = 45$ min) in lateral tibiofemoral cartilage. Tibial cartilage is severely damaged (black arrow) as well as a cyst in the subchondral bone is seen under the damaged cartilage (white arrow). In the femur, a localized sclerotic area is found (red arrow).**

VOIs of tibia (TLC and TMC), vBMDs of SB and TB correlated negatively with the cartilage thickness ($\rho = -0.501$, $p = 0.003$ and $\rho = -0.457$, $p = 0.007$, respectively). No significant correlations were found in other anatomical regions or when combining all the regions (Table 2). In addition to the quantitative findings, cartilage and bone changes could be detected visually in the contrast-enhanced images (Fig. 5).

DISCUSSION

The contrast-enhanced imaging of human knee joints with a clinical CBCT scanner enabled the simultaneous detection of subchondral bone defects (e.g. cysts, sclerosis) and cartilage lesions, and hence enabled ICRS scoring. Furthermore, quantitative parameters (i.e., vBMD, cartilage and SBP thickness,

and normalized attenuation in cartilage) could be simultaneously determined. Thus, dCBCTa provided a feasible method to detect characteristic pathological changes related to knee joint OA also enabling the localization of the fissures in the cartilage. vBMD of SBP was found to depend on the severity of cartilage injury in adjacent tissue, both damaged and severely damaged tissues being distinguishable from less intact tissue or tissue with minor damage (Fig. 3). However, no significant relationship between the normalized attenuation in cartilage and subchondral bone vBMD was found (Table 2). This suggests that the normalized attenuation is already affected by early cartilage tissue changes whereas change in vBMD of SBP might occur after change in the mechanical properties of cartilage. This indicates a slower process of bone remodeling in the SBP,[8] whereas changes in cartilage composition may be more instant when related to injury.

Normalized attenuation in cartilage ($t = 45$ min) was significantly related to ICRS grade of the adjacent lesion (Fig. 4). In earlier studies, having a low number of subjects with severe (ICRS ≥ 3) cartilage injuries, no significant association between X-ray attenuation in cartilage and ICRS grade was found.[11,16] Despite of the significant trend in normalized attenuation values versus ICRS scores, no statistically significant differences were found between the consecutive ICRS scores, e.g. when comparing ICRS = 1 and ICRS = 2 in the current study. Due to limited number of samples, we could not conduct the analyses site-specifically. In the future, with higher number of patients, these differences could be investigated by conducting site-specific analyses.

Diffusion of anionic contrast agent through deeper layers of intact cartilage is slower than at more superficial tissue.[29] However, although cartilage VOIs with lesions were thinner and partially comprised only the deepest cartilage layer, transfer of the contrast

agent into cartilage was greater in VOIs with injury than in the intact cartilage or in cartilage with minor damage (Fig. 2). As the contrast agent intake in the deep cartilage below the lesion is presumably less in fresh lesions than in mature ones, properties of deep cartilage under the lesion may have undergone major changes (i.e., PG loss and disruption of the collagen network). The depth-dependent differences in contrast agent diffusion may, however, induce variation in results and may need to be considered in future studies. The dCBCTa is not able to distinguish whether the changes in diffusion are related to disruption of collagen network or PG depletion when anionic contrast agent is used. Indeed, both tissue changes may induce similar response in contrast agent intake. However, since both changes are characteristic signs for early tissue degeneration, the increased diffusion of the used anionic contrast agent is suggested to provide a robust indicator for cartilage changes in early OA.

The normalized attenuation in cartilage varied among the anatomical sites (Fig. 2). This may be due to differences in cartilage composition in different anatomical areas.[1] Variation in cartilage thickness also contributes to this finding as the contrast agent diffusion depends on the distance (i.e., thickness) according to Fick's second law of diffusion.[9] Additionally, the uneven distribution of contrast agent in the joint capsule may partially have contributed to the detected site dependency. To minimize this possibility, the injections of contrast agent were conducted carefully by experienced clinicians. Based on the previous studies[13,16], 40 ml of contrast agent dilution (160 mg iodine/mL) was injected either through the superolaterar or anterolaterar portal into joint space. Both injection sites enabled the distribution of the contrast agent in the whole joint space. In addition, to ensure even distribution of the contrast agent in the synovial fluid, patients flexed their legs several times immediately after the injection. Furthermore, the X-ray attenuation of the cartilage was normalized with that of the adjacent SF VOI, thus minimizing the effect of uneven distribution of contrast agent. A previous study also suggests that diffusion properties of ioxaglate were independent of its concentration outside the cartilage.[28] Despite these facts, high site-to-site variation in normalized attenuation in this study suggests that if the normalized attenuation is utilized as a diagnostic parameter, site-specific threshold values for pathological findings could be set.

Interaction of bone and cartilage tissues is evident in OA development.[19] Nevertheless, no consensus on the sequence of alterations in subchondral bone and cartilage during OA progress or cartilage lesions exists. Early stage OA may involve microcracks or subchondral bone resorption leading to diminishing of the subchondral plate.[3,19] On the other hand, stiffening of subchondral bone has been suggested as a precondition for the OA progress.[24] In the present study, the changes in the subchondral bone plate found are consistent with the latter theory, suggesting that lesion severity increases vBMD in subchondral plate. However, the vBMD changes might follow the increased stresses on bone after cartilage degeneration and decrease in PG content. The increase in vBMD and thickening of SBP were also found to relate with each other. In previous studies, similar relation was found in bovine tibial plateau[1] and human metacarpal.[18] However, the relationship between SBP thickness and density needs further evaluation with sophisticated techniques[31] to confirm that the connection is truly related to physiological alterations. Cartilage injuries were not associated to SB or TB mineral densities but when considering only tibial VOIs, TLC and TMC, SB and TB mineral densities correlated negatively with cartilage thickness. In a previous study, similar negative correlation was found.[4] Moreover, the finding was suggested to predict the progress of OA.

Our previous study showed that when combined with hydroxyapatite phantoms, CBCT enables detection of volumetric distribution of BMD in a knee joint.[32] In that study, vBMD values determined with CBCT and CT scanners correlated although the values were found to differ considerably. Similar BMD values in our previous (without contrast agent) and present (with contrast agent) studies suggest that the presently applied contrast agent induces no significant artefacts in the image that would hinder the assessment of the bone. Due to the moderate signal-to-noise ratio, CBCT was shown to be applicable method to detect subtle to severe alterations in cartilage and subchondral bone (e.g., osteochondral sclerosis and cysts, Fig. 5). As a limitation, accurate determination of thin structures such as SBP from CBCT images are compromised by image blurring and partial volume effect.[23,31] However, the effect of these artefacts were reduced by using only the interior voxels of SBP for determining the BMD, which are less affected by image blurring and partial volume effect. Furthermore, the resolution achieved with the imaging method may be too low to detect the very finest changes in the cartilage. However, due to technical developments, resolution and signal-to-noise ratio of CBCT are improving, increasing the sensitivity and accuracy of the imaging, while the radiation dose remains low. Regardless of the low dose, the development of techniques that require only one acquisition should be considered.

Since the age of study subjects varied, statistical analyzes (i.e., Mixed Model) that consider a patient dependency were used. Then, the alterations were found to be lesion severity dependent. In the future, a

study involving clearly separate age groups would allow further evaluation of the age dependency of cartilage and bone properties. In the present study, the type of a joint injury, e.g., meniscus or cruciate ligament injuries, was not taken into account. When aiming to improve OA diagnostics and the prediction of its progress, they have to be accounted. Interestingly, our recent study suggested that contrast-enhanced CBCT imaging also enables the detection of meniscal pathologies.[12]

As a limitation of the present study, no MRI reference was available to validate the lesions. A previous study, however, showed a strong correlation ($\rho = 0.69$, $p < 0.01$) between the ICRS scorings based on CBCT arthrographic and MR images.[16] In addition, contrast-enhanced CT has been shown to have potential to detect fresh cartilage injuries *in vitro*.[14] Utilizing mixture of diffusive and non-diffusive contrast agents could be an advantageous way to detect lesions and post-traumatic changes in surrounding tissue. However, thorough *in vitro*, *ex vivo*, and biocompatibility studies are required before introducing a novel method for clinical practice. In dCBCTa, the contrast agent is injected intra-articularly, similarly as in clinical MR imaging of the rotator cuff of the shoulder, whereas in dGEMRIC the contrast agent is injected intravenously. Therefore, both imaging methods, dCBCTa and dGEMRIC, can be considered invasive. Despite of the invasiveness, the present patients did not report feeling the imaging procedure to be uncomfortable. Utilization of undiluted hypertonic contrast agents (i.e., Hexabrix™ of full strength, 320 mg iodine/ml) temporarily softens the cartilage and, theoretically, makes it vulnerable to mechanical damage.[33] Nevertheless, this risk was minimized since the present imaging protocol included no weight bearing exercise but flexing the leg in a sitting position. Further, the injected contrast agent was diluted to half of the original concentration and it excretes from the joint space in a couple of hours.[13] Moreover, dCBCTa enables imaging with a half shorter delay (45 min) compared to that in dGEMRIC. Therefore, for practical and logistical reasons, it may be better suited for clinical use.

The aim of the current study was to evaluate whether the presented imaging method can be utilized to detect OA initiated changes in the cartilage and subchondral bone. The segmentations were done manually since, based on the authors' knowledge, no fully automatic method exists for reliable segmentation of cartilage in contrast-enhanced CT images. To minimize possible bias, segmentations were carefully conducted considering all three orthogonal image planes. In the future, development of fully automatic segmentation and analysis tools are of utmost importance for clinical adoption of this technique.

In conclusion, the results of the present study suggest that clinical dCBCTa, when conducted using anionic contrast agent and hydroxyapatite phantoms, enables the quantitative *in vivo* analysis of both articular cartilage and subchondral bone. The simultaneous detection of chondral injuries and condition of surrounding cartilage, as well as changes in subchondral bone vBMD, could improve the diagnostics of the first signs of post-traumatic OA. Furthermore, the method and findings of this study may be utilized when constructing a realistic computational model to evaluate the effects of inter-related changes in cartilage and subchondral bone on joint function and development of OA.[20,34]

CONFLICT OF INTEREST

Authors declare no conflicts of interest.

REFERENCES

[1]Aula, A. S., J. S. Jurvelin, and J. Töyräs. Simultaneous computed tomography of articular cartilage and subchondral bone. *Osteoarthr. Cartil.* 17:1583–1588, 2009.

[2]Bennell, K. L., M. W. Creaby, T. V. Wrigley, and D. J. Hunter. Tibial subchondral trabecular volumetric bone density in medial knee joint osteoarthritis using peripheral quantitative computed tomography technology. *Arthritis Rheum.* 58:2776–2785, 2008.

[3]Botter, S. M., G. J. V. M. van Osch, J. H. Waarsing, J. C. van der Linden, J. A. N. Verhaar, H. A. P. Pols, J. P. T. M. van Leeuwen, and H. Weinans. Cartilage damage pattern in relation to subchondral plate thickness in a collagenase-induced model of osteoarthritis. *Osteoarthr. Cartil.* 16:506–514, 2008.

[4]Bruyere, O., C. Dardenne, E. Lejeune, B. Zegels, A. Pahaut, F. Richy, L. Seidel, O. Ethgen, Y. Henrotin, and J.-Y. Reginster. Subchondral tibial bone mineral density predicts future joint space narrowing at the medial femorotibial compartment in patients with knee osteoarthritis. *Bone* 32:541–545, 2003.

[5]Buckwalter, J. A. Articular cartilage injuries. *Clin. Orthop. Relat. Res.* 402:21–37, 2002.

[6]Buckwalter, J. A., and H. J. Mankin. Articular cartilage: degeneration and osteoarthritis, repair, regeneration, and transplantation. *Instr. Course Lect.* 47:487–504, 1998.

[7]Buckwalter, J. A., J. L. Marsh, T. Brown, A. Amendola, and J. A. Martin. Articular cartilage injury. In: Principles of Tissue Engineering, edited by R. Lanza, R. Langer, and J. P. Vacanti. New York: Elsevier, 2014, pp. 1253–1266.

[8]Burr, D. B., and M. A. Gallant. Bone remodelling in osteoarthritis. *Nat. Rev. Rheumatol.* 8:665–673, 2012.

[9]Crank, J. The Mathematics of Diffusion. Oxford: Oxford University Press, 1979.

[10]Goldring, M. B., and S. R. Goldring. Articular cartilage and subchondral bone in the pathogenesis of osteoarthritis. *Ann. N. Y. Acad. Sci.* 1192:230–237, 2010.

[11]Hirvasniemi, J., K. A. M. Kulmala, E. Lammentausta, R. Ojala, P. Lehenkari, A. Kamel, J. S. Jurvelin, J. Töyräs, M. T. Nieminen, and S. Saarakkala. *In vivo* comparison of delayed gadolinium-enhanced MRI of cartilage and delayed quantitative CT arthrography in imaging of articular cartilage. *Osteoarthr. Cartil.* 21:434–442, 2013.

[12]Honkanen, J. T. J., E. K. Danso, J.-S. Suomalainen, V. Tiitu, R. K. Korhonen, J. S. Jurvelin, and J. Töyräs. Contrast enhanced imaging of human meniscus using cone beam CT. *Osteoarthr. Cartil.* 23:1367–1376, 2015.

[13]Kokkonen, H. T., A. S. Aula, H. Kröger, J.-S. Suomalainen, E. Lammentausta, E. Mervaala, J. S. Jurvelin, and J. Töyräs. Delayed computed tomography arthrography of human knee cartilage *in vivo*. *Cartilage* 3:334–341, 2012.

[14]Kokkonen, H. T., J. S. Jurvelin, V. Tiitu, and J. Töyräs. Detection of mechanical injury of articular cartilage using contrast enhanced computed tomography. *Osteoarthr. Cartil.* 19:295–301, 2011.

[15]Kokkonen, H. T., J. Mäkelä, K. A. M. Kulmala, L. Rieppo, J. S. Jurvelin, V. Tiitu, H. M. Karjalainen, R. K. Korhonen, V. Kovanen, and J. Töyräs. Computed tomography detects changes in contrast agent diffusion after collagen cross-linking typical to natural aging of articular cartilage. *Osteoarthr. Cartil.* 19:1190–1198, 2011.

[16]Kokkonen, H. T., J. Suomalainen, A. Joukainen, H. Kröger, J. Sirola, J. Jurvelin, J. Salo, and J. Töyräs. *In vivo* diagnostics of human knee cartilage lesions using delayed CBCT arthrography. *J. Orthop. Res.* 32:403–412, 2014.

[17]Kulmala, K. A. M., H. M. Karjalainen, H. T. Kokkonen, V. Tiitu, V. Kovanen, M. J. Lammi, J. S. Jurvelin, R. K. Korhonen, and J. Töyräs. Diffusion of ionic and non-ionic contrast agents in articular cartilage with increased cross-linking-contribution of steric and electrostatic effects. *Med. Eng. Phys.* 35:1415–1420, 2013.

[18]Lakin, B. A., D. J. Ellis, J. S. Shelofsky, J. D. Freedman, M. W. Grinstaff, and B. D. Snyder. Contrast-enhanced CT facilitates rapid, non-destructive assessment of cartilage and bone properties of the human metacarpal. *Osteoarthr. Cartil.* 23:2158–2166, 2015.

[19]Li, G., J. Yin, J. Gao, T. S. Cheng, N. J. Pavlos, C. Zhang, and M. H. Zheng. Subchondral bone in osteoarthritis: insight into risk factors and microstructural changes. *Arthritis Res. Ther.* 15:223, 2013.

[20]Mononen, M. E., P. Tanska, H. Isaksson, and R. K. Korhonen. A novel method to simulate the progression of collagen degeneration of cartilage in the knee: data from the osteoarthritis initiative. *Sci. Rep.* 6:21415, 2016.

[21]Mow, V. C., A. Ratcliffe, and A. Robin. Poole. Cartilage and diarthrodial joints as paradigms for hierarchical materials and structures. *Biomaterials* 13:67–97, 1992.

[22]Muraoka, T., H. Hagino, T. Okano, M. Enokida, and R. Teshima. Role of subchondral bone in osteoarthritis development: a comparative study of two strains of guinea pigs with and without spontaneously occurring osteoarthritis. *Arthritis Rheum.* 56:3366–3374, 2007.

[23]Prevrhal, S., J. C. Fox, J. A. Shepherd, and H. K. Genant. Accuracy of CT-based thickness measurement of thin structures: modeling of limited spatial resolution in all three dimensions. *Med. Phys.* 30:1–8, 2003.

[24]Radin, E. L., and R. M. Rose. Role of subchondral bone in the initiation and progression of cartilage damage. *Clin. Orthop. Relat. Res.* 213:34–40, 1986.

[25]Roberts, J. A., N. A. Drage, J. Davies, and D. W. Thomas. Effective dose from cone beam CT examinations in dentistry. *Br. J. Radiol.* 82:35–40, 2009.

[26]Román-Blas, J. A., S. Castañeda, R. Largo, and G. Herrero-Beaumont. Subchondral bone remodelling and osteoarthritis. *Arthritis Res. Ther.* 14:A6, 2012.

[27]Silvast, T. S., J. S. Jurvelin, M. J. Lammi, and J. Töyräs. pQCT study on diffusion and equilibrium distribution of iodinated anionic contrast agent in human articular cartilage—associations to matrix composition and integrity. *Osteoarthr. Cartil.* 17:26–32, 2009.

[28]Silvast, T. S., J. S. Jurvelin, V. Tiitu, T. M. Quinn, and J. Töyräs. Bath concentration of anionic contrast agents does not affect their diffusion and distribution in articular cartilage *in vitro*. *Cartilage* 4:42–51, 2012.

[29]Silvast, T. S., H. T. Kokkonen, J. S. Jurvelin, T. M. Quinn, M. T. Nieminen, and J. Töyräs. Diffusion and near-equilibrium distribution of MRI and CT contrast agents in articular cartilage. *Phys. Med. Biol.* 54:6823–6836, 2009.

[30]Spahn, G., H. M. Klinger, and G. O. Hofmann. How valid is the arthroscopic diagnosis of cartilage lesions? Results of an opinion survey among highly experienced arthroscopic surgeons. *Arch. Orthop. Trauma Surg.* 129:1117–1121, 2009.

[31]Treece, G. M., A. H. Gee, P. M. Mayhew, and K. E. S. Poole. High resolution cortical bone thickness measurement from clinical CT data. *Med. Image Anal.* 14:276–290, 2010.

[32]Turunen, M. J., J. Töyräs, H. T. Kokkonen, and J. S. Jurvelin. Quantitative evaluation of knee subchondral bone mineral density using cone beam computed tomography. *IEEE Trans. Med. Imaging* 34:2186–2190, 2015.

[33]Turunen, M. J., J. Töyräs, M. J. Lammi, J. S. Jurvelin, and R. K. Korhonen. Hyperosmolaric contrast agents in cartilage tomography may expose cartilage to overload-induced cell death. *J. Biomech.* 45:497–503, 2012.

[34]Venäläinen, M. S., M. E. Mononen, S. P. Väänänen, J. S. Jurvelin, J. Töyräs, T. Virén, and R. K. Korhonen. Effect of bone inhomogeneity on tibiofemoral contact mechanics during physiological loading. *J. Biomech.* 49:1111–1120, 2016.

[35]Yamada, K., R. Healey, D. Amiel, M. Lotz, and R. Coutts. Subchondral bone of the human knee joint in aging and osteoarthritis. *Osteoarthr. Cartil.* 10:360–369, 2002.